The Effect of Various Parameters on Dry Sliding Wear Behavior and Subsurface of Aged Hybrid Metal Matrix Composites Using Taguchi Technique

B. M. Viswanatha[1*], M. Prasanna Kumar[2], S. Basavarajappa[2] and T. S. Kiran[1]

* *vishwanathabm@gmail.com*

Received: April 2016 Accepted: April 2017

[1] Department of Mechanical Engineering, Kalpataru Institute of Technology, Tiptur, India.
[2] Department of studies in Mechanical Engineering, University BDT College of Engineering, Davangere, India.
DOI: 10.22068/ijmse.14.2.71

Abstract: *The effects of applied load, sliding speed and sliding distance on the dry sliding wear behavior of aged Al-SiC_p-Gr composites were investigated. The specimen were fabricated by stir-casting technique. The pin-on-disc wear testing machine was used to investigate the wear rate by design of experiments based on L_{27} using Taguchi technique. Sliding distance was the most important variable that influenced the wear rate followed by sliding speed and applied load. The worn out surfaces were analyzed by SEM and EDS to study the subsurface mechanism of wear. The addition of reinforcements showed improved tribological behavior of the composite than base alloy.*

Keywords: *Composites, Aged, Wear, Subsurface, Taguchi Technique.*

1. INTRODUCTION

Aluminium Metal Matrix Composites (AMMCs) are prominent material to attain high specific strength, high stiffness, low density and good wear resistance compared to the monolithic materials. These are potential replacements for conventional materials in automobile and aerospace applications [1-2]. Several researchers have worked on the improvement of the tribological properties of AMMCs by addition of single ceramic particles viz., SiC_p, Al_2O_3, Gr etc. A few researchers have carried out the research using the combination of the above reinforcements. Increase in the content of SiC_p in aluminium matrix material exhibits good wear resistance. Tjong et al. [3] worked on wear behavior of Al-12% Si alloy reinforced with low volume fraction of SiC_p. The results showed that the addition of low volume fraction of SiC_p is very effective in increasing the wear resistance. Pramila Bai et al. [4] studied the dry sliding wear test of A356 reinforced with 15-25 wt. % of SiC_p. The result revealed that, increase in the content of SiC_p reduced wear.

Ravikiran and Surappa [5] studied the wear behaviour of A356-30 wt. % SiC_p composite as a function of sliding speed. The wear rate of specimen decreases with increasing speed, as the SiC_p is exposed to the specimen surface is increased. Natarajan et al. [6] studied the wear behavior of A356-25SiC_p sliding against automobile friction material. They concluded that the wear rate of MMCs was lower than the cast iron. That makes it a suitable material for brake rotor applications. Wilson and Alpas [7] studied the wear mechanism of A356 alloy and A356-20SiC_p composite. They reported that the addition of SiC_p to A356 aluminium alloy leads to mild wear regime at higher speed and loads, there by inhibiting sever wear. The SiC_p assists the retention of oxide transfer layer on composite sliding surface. It prevents metal to metal contact and keeps wear behavior within the mild wear regime.

The graphite (Gr) used as second reinforcement has to a possible reduction of friction, as solid lubricant imparts good wear resistance to the composites [8]. Akhlaghi and Bidaki [9] studied the effects of addition of lower wt. % (2-5 wt. %) of Gr which exhibited good wear resistance against a higher wt. % (5-20 wt. %) of Gr. Yang et al. [10] studied the tribological properties of A356 alloy with varying Gr of 2, 4, 6 and 8 wt. %. The result showed that 4 and 6 wt. % of Gr particles exhibit

[Downloaded from railway.iust.ac.ir on 2024-10-10]

[DOI: 10.22068/ijmse.14.2.71]

lowest wear compared to the 8 wt. %, but sliding speed and normal load had negligible influence on wear rate. Liu et al. [11] studied the wear resistance of Al-Si-Gr composites aged at different temperatures. The wear resistance of aged composites showed better results than as-cast matrix material. Rajaram et al. [12] studied the wear properties of Al-Si alloy reinforced with 3 wt. % of Gr at elevated temperatures. They concluded that, an increase in addition of Gr improved the tribological behaviour when compared with the base alloy.

The addition of SiC_p to Al alloy increases both mechanical and wear resistance but makes machining difficult [13]. The addition of SiC_p along with Gr particles helps to retain the property and reduces the problem of machining. Al matrix reinforced with SiC_p and Gr forms Al-SiC-Gr hybrid composites that improves the tribological characteristics when compared with the base alloy. SiC_p imparts strength and wear resistance, while Gr acts as a solid lubricant [14]. Basavarajappa et al. [15] studied the influence of sliding speed on the extent of subsurface damage on Al-15SiC_p and Al-15SiC_p-3Gr composites. Increasing the sliding speed increases the degree of subsurface deformation.The degree of subsurface deformation and wear rate in Gr composites is less than that of free Gr composites. Suresha and Sridhara [16] reported that the combination of reinforcements of SiC_p and Gr showed better wear behaviour than SiC_p alone. Ames and Alpas [17] studied the wear mechanism of A356 aluminium alloy reinforced with SiC_p and Gr. The wear rate of hybrid composites is significantly lower than the wear rate of base alloy at low and medium loads. Riahi and Alpas [18] observed that the combination of A356-10SiC_p-4Gr revealed good wear resistance than A356-5Al_2O_3-3Gr composites.

Gomez et al. [19] studied the advantage of heat treatment on wear resistance of A6069-SiC_p composite material. It was found that, the heat treated MMCs at T6-7 hrs showed maximum hardness and superior wear résistance. Lin et al. [20] studied the hardness and dry sliding wear of T6 heat treated Al6061-Gr composites and A6069. The tribological characteristic depends on hardness and rate of releasing of Gr particles from the composite specimen. Benal and Shivananad [21] studied the wear characteristics of aged Al6061 hybrid composites. At an aging duration of 5 hrs the composites showed maximum wear resistance. Viswanatha et al. [22] studied the effect of ageing duration on wear behaviour of the aluminium hybrid composites. From the results, A356-9SiC_p-3Gr composites aged at T6-9 hrs showed better mechanical and tribological properties when compared to the base alloy.

Mahdavi and Akhlaghi [23] studied the hardness and tribological behaviour of aged Al6061-SiC_p-Gr composites. The results revealed that hardness of the composites increases with addition of reinforcements. Al-20SiC_p-9Gr gives better tribological property when compared to the other tested specimens. Venkataraman amd Sunderarajan [24] studied the formation of mechanical mixed layer (MML) and its effect of mechanism on wear rate. The MML plays a vital role on the wear behaviour of the composite specimen. The MML protects the surface of specimen from critical sliding conditions. Kiran et al. [25] studied the dry sliding wear behavior of zinc based alloy and composites and the effect of parameters on wear which were investigated using Taguchi technique. Applied load was the most significant parameter to influence the wear volume loss. Dharmalingam et al. [26] investigated the wear parameters by Taguchi method coupled with gray relation analysis to find the performance characteristics. The order of significance on wear rate was wt. % of molybdenum-disulfide followed by sliding velocity and applied load. Sahin [27] optimized the wear behavior of SiC_p reinforced MMCs with two different particles size by Taguchi method. The composite with smaller particle size exhibits severe wear due to easy removal of particles from the matrix. While the larger particles fractured and formed a MML on the surface revealing superior wear resistance. Ravindran et al. [28-30] investigated the effect of applied load, sliding speed and sliding distance on the friction and wear behavior of hybrid composites by Taguchi method. The wear rate increased with an increase in sliding distance and applied load but decreased with increase of Gr content. The most common

[Downloaded from railway.iust.ac.ir on 2024-10-10]

[DOI: 10.22068/ijmse.14.2.71]

method of manufacturing process of MMCs are stir cast technique [31-32].

In view of the above literature review, limited works have been carried out to study the effect of ageing on the dry sliding wear behaviour of the composites. The main objective of the investigation was to study the effect of sliding distance, sliding speed and applied load on wear behaviour of base alloy and hybrid composites using Taguchi technique. Taguchi technique is a powerful tool for the design of high quality systems. The Taguchi approach to experimentation provides an orderly way to collect, analyze and interpret data to satisfy the objectives. By using this method, in the Design of Experiments (DOE), one can obtain the maximum amount of information for the amount of experimentation conducted. Taguchi parameter design can optimize the performance characteristics through the setting of design parameters and reduce the sensitivity of the system performance to the source of variation. This is accomplished by the efficient use of experimental runs to the combinations of variables studied. Taguchi technique creates a standard orthogonal array to accommodate the effect of several factors on the target value and defines the plan of experiments. The experimental results are analyzed using analysis of means and variance to study the influence of factors on wear [29]. In addition, the scanning electron microscope (SEM) and electron dispersive spectroscopy (EDS) of worn out surfaces were analysed to know the wear mechanisms.

2. EXPERIMENTAL PROCEDURE

2. 1. Material Fabrication

Fabrication of the base alloy (A356) and composites (A356-9SiC_p-3Gr) was carried out using stir-cast technique. A356 was melted in graphite crucible in an automatic temperature controlled furnace. During the fabrication, 1 wt. % of magnesium (Mg) was added to the liquid metal in order to achieve good bonding between the matrix and reinforcement. The reinforcements were pre-heated to oxidize the surface. The pre-heated reinforcements were added to the stirred liquid metal and the processing temperature was maintained at 750ºC with stirring speed of 500 rpm. The molten metal was poured into the mould box which was pre-heated to avoid the defects like pores and cavities in the specimen. T6–heat treatment was carried-out for the wear specimens at 540ºC for 12 hours and is quenched in 60ºC water. The heat treated

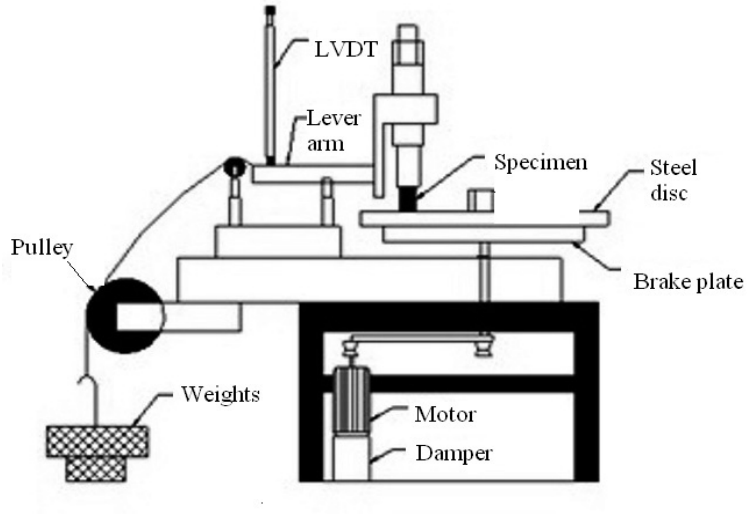

Fig. 1. Pin on disc wear testing machine

[Downloaded from railway.iust.ac.ir on 2024-10-10]

[DOI: 10.22068/ijmse.14.2.71]

specimens were aged at 155°C for 9 hours and is quenched in 60°C water.

2. 2. Experimental Procedure

The microstructure and hardness of the specimen was evaluated using Vicker hardness test. The wear testing was carried out on DUCOM pin-on-disc machine to evaluate the dry sliding wear behavior of the composites as shown in Figure 1. The tests were performed as per ASTM G99-95 standard. The cast specimen were turned and polished metallographically for a size of 8 mm diameter and 30 mm height.

The specimen was cleaned with acetone and initial mass was measured using electronic weighing machine with least count of 0.0001g. The specimen was pressed against the rotating EN-32 steel disc with hardness of 65 HRC. The tests were carried out by varying applied load, sliding speed and sliding distance. At the end of each test, the final mass of the specimen was measured. The mass loss was calculated by the difference between the initial and final mass of the specimen. The volume loss was calculated using corresponding density values of the specimen. The wear rate of the specimen was calculated using the ratio of volume loss to corresponding sliding distance. The subsurface of worn out surface was analyzed using SEM. The wear test specimen was cut along its diameter, perpendicular to the specimen surface. The cut surface was polished metallographically to observe the surface behavior (JEOL, JSM-6360).

2. 3. Design of experiment

In the present work, L_{27} orthogonal array (OA) was selected that has 27 rows and 13 columns as shown in Table 1. The experiment consists of 27 tests (each row in the L_{27} OA) and columns are assigned to the parameters. The first column is assigned for applied load (L), second column for sliding speed (S), fifth column for sliding distance (D) and the remaining columns were assigned to the interactions. The experiments were conducted on three parameters at three levels by Taguchi technique. The design parameters with levels are listed in Table 3.7. The desired performance response was calculated by analysis of variance (ANOVA). The main effect plot, interaction plots and regression model were generated. The wear response was conducted with the objective of smaller-the-best.

3. RESULTS

The objective of the present investigation is to evaluate the wear rate of A356 alloy and A356-9SiC_p-3Gr composite by Taguchi method. Both the specimen were heat treated and aged at 9 hours. The parameters applied load, sliding speed, sliding distance and interaction of all variables were studied.

3. 1. Microstructure and Hardness

The particle reinforced composite plays a significant role in the overall strength of the composite. The increase in strength of the matrix invariably enhances the mechanical properties of the composite. Due to this reason the age hardenable base alloy was considered. The heat treatment of base alloy resulted in the removal of dendritic structure and formation of uniform equiaxed grainstructure. The precipitation along the grain boundaries and within the grains are noted to be much finer. However further ageing was carriedout for 9 hrs at 155°C which leads to dissolution of eutectic phase and formation of uniform distribution of fine intermetallic precipitates in the matrix (Fig. 2a). As a result, reinforcements are uniformly distributed within the matrix (Fig. 2b) and produces a maximum hardness (Table 3).

Further increase in the strength of the base alloy by addition of reinfocrements was observed. In composites, reinforcements (SiC_p and Gr) leads to mismatch in thermal stress in the surrounding matrix resulting in increase in dislocation density which increases the precipitation characteristics. The strength was increased due to age hardening in order to develop the acceptable properties. Increase in hardness of the composite was noticable when compared to the base alloy, because of addition of 9 wt. % of SiC_p to the A356-3Gr composites.

The ageing was a phenomenon of precipitation, which is dictated by the combined

[Downloaded from railway.iust.ac.ir on 2024-10-10]

[DOI: 10.22068/ijmse.14.2.71]

Table 1. L_{27} Orthogonal array of Taguchi technique

L_{27}, test	1	2	3	4	5	6	7	8	9	10	11	12	13
1	1	1	1	1	1	1	1	1	1	1	1	1	1
2	1	1	1	1	2	2	2	2	2	2	2	2	2
3	1	1	1	1	3	3	3	3	3	3	3	3	3
4	1	2	2	2	1	1	1	2	2	2	3	3	3
5	1	2	2	2	2	2	2	3	3	3	1	1	1
6	1	2	2	2	3	3	3	1	1	1	2	2	2
7	1	3	3	3	1	1	1	3	3	3	2	2	2
8	1	3	3	3	2	2	2	1	1	1	3	3	3
9	1	3	3	3	3	3	3	2	2	2	1	1	1
10	2	1	2	3	1	2	3	1	2	3	1	2	3
11	2	1	2	3	2	3	1	2	3	1	2	3	1
12	2	1	2	3	3	1	2	3	1	2	3	1	2
13	2	2	3	1	1	2	3	2	3	1	3	1	2
14	2	2	3	1	2	3	1	3	1	2	1	2	3
15	2	2	3	1	3	1	2	1	2	3	2	3	1
16	2	3	1	2	1	2	3	3	2	1	2	3	1
17	2	3	1	2	2	3	1	1	2	3	3	1	2
18	2	3	1	2	3	1	2	2	3	1	1	2	3
19	3	1	3	2	1	3	2	1	3	2	1	3	2
20	3	1	3	2	2	1	3	2	1	3	2	1	3
21	3	1	3	2	3	2	1	3	2	1	3	2	1
22	3	2	1	3	1	3	2	2	1	3	3	2	1
23	3	2	1	3	2	1	3	3	2	1	1	3	2
24	3	2	1	3	3	2	1	1	3	2	2	1	3
25	3	3	2	1	1	3	2	3	2	1	2	1	3
26	3	3	2	1	2	1	3	1	3	2	3	2	1
27	3	3	2	1	3	2	1	2	1	3	1	3	2

effect of time and temperature. The precipitation kinetics are strongly influenced by the durations. The similar phenomenon is observed by earlier researcher [37].

3. 2. Statistical Analysis of ANOVA

L27 array was selected and it has 27 rows as shown in Table 4. The wear parameters taken for the experiments are (i) applied load (ii) sliding

[Downloaded from railway.iust.ac.ir on 2024-10-10]

[DOI: 10.22068/ijmse.14.2.71]

Table 2. Design parameter with levels

Level	Load L (N)	Sliding velocity S (m/s)	Sliding Distance D (m)
1	10	200	1500
2	30	500	3000
3	50	800	4500

Table 3. Hardness of the specimens

Specimen	Composition	Hardness (VHN)
1	A356	94
2	A356-9SiC$_p$-3Gr	144

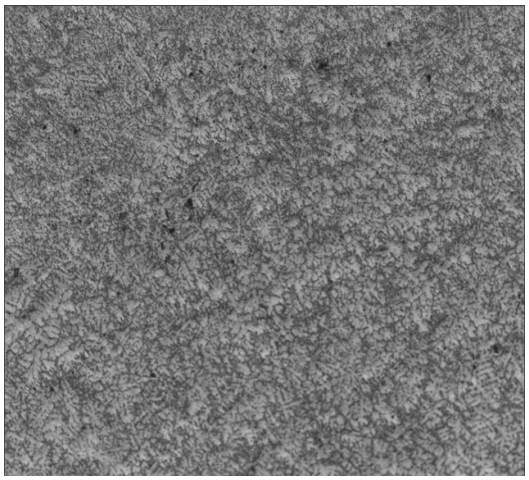

2. (a)

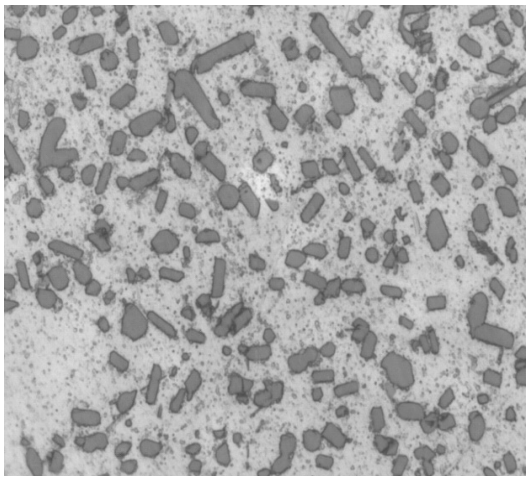

2. (b)

Fig. 2. Microstructure of (a). A356 alloy (b). A356-9SiC$_p$-3Gr

speed and (iii) sliding distance. The experiment consists of 27 tests and columns are assigned with the parameters. The first column is for applied load (L), second column is for sliding speed (S), fifth column was assigned to sliding distance (D) and remaining columns were assigned to the interactions. The results of ANOVA for wear rate of base alloy and composites are tabulated in Table 5 and 6 respectively.

F-ratio is calculated by ANOVA, also called as ratio between regression mean square and mean error term. This ratio is important to find the significance of the parameters under the investigation with consideration of all variance and error term at desired significant level. Increased value of F accordingly increases the significance of the parameter shows the contribution of individual parameters such as D, S and L and also interaction of parameters such as S*D, S*L and D*L that influence on wear rate of the materials. From Table 5, sliding distance (P=56.81%) has more contribution to wear rate when compared with the other two parameters sliding speed (P=21.21%), applied load (17.25%) and negligible contribution of interaction D*L (P=1.11%). The effect of interaction is less significant in case of base alloy. Table 6 shows that sliding distance (P= 53.49%) exhibits higher influence on wear rate followed by sliding speed (P=20.21%) and applied load (P=18.32%). Their was no interaction effect on the wear rate of composites. Thus, the distance has predominant effect on wear rate compared to sliding speed and applied load for both base alloy and composite.

[Downloaded from railway.iust.ac.ir on 2024-10-10]

[DOI: 10.22068/ijmse.14.2.71]

Table 4. Orthogonal array of Taguchi and experimental results

Expt. No.	Load, L (N)	Sliding speed, S (m/s)	Sliding distance, D (m)	Wear Rate ($mm^3/m*10^{-3}$), A356	Wear Rate ($mm^3/m*10^{-3}$), A356-9SiC$_p$-3Gr
1	10	1.25	1500	11.5	1.8
2	10	1.25	3000	13.4	3.7
3	10	1.25	4500	16.8	5.4
4	30	1.25	1500	12.7	2.1
5	30	1.25	3000	14.4	4.5
6	30	1.25	4500	18.1	6.3
7	50	1.25	1500	13.2	3.6
8	50	1.25	3000	16.8	5.4
9	50	1.25	4500	20.6	7.4
10	10	3.14	1500	13.4	2.3
11	10	3.14	3000	15.8	5.61
12	10	3.14	4500	17.9	7.1
13	30	3.14	1500	13.9	2.8
14	30	3.14	3000	16.9	5.9
15	30	3.14	4500	19.9	7.6
16	50	3.14	1500	14.8	4.7
17	50	3.14	3000	19.9	9.1
18	50	3.14	4500	21.7	10.1
19	10	5.02	1500	14.8	3.8
20	10	5.02	3000	16.2	6.1
21	10	5.02	4500	20.2	8.7
22	30	5.02	1500	15.8	3.9
23	30	5.02	3000	18.5	6.8
24	30	5.02	4500	22.4	9.3
25	50	5.02	1500	17.2	6.1
26	50	5.02	3000	21.5	10.7
27	50	5.02	4500	24.8	11.6

[Downloaded from railway.iust.ac.ir on 2024-10-10]

[DOI: 10.22068/ijmse.14.2.71]

Table 5. ANOVA of A356 alloy of wear rate

Factors	SS	DOF	Mean Sq.	T.F.	F	%P
L	52.20	2	26.10	39.60	317.08	17.25
D	168.82	2	84.41	128.09	1025.47	56.81
S	63.85	2	31.92	48.44	387.84	21.21
D*L	5.92	4	1.48	2.24	17.99	1.11
S*L	1.17	4	0.29	0.44	3.55	-
S*D	2.18	4	0.54	0.82	6.63	-
Pooled Error	0.65	8	0.65			3.59
Total	294.808		144.7556			100

S=0.534928, R-Sq=98.1% and R-Sq (adj) =97.5%

Table 6. ANOVA of A356-9SiC_p-3Gr-9hrs of wear rate

Factors	SS	DOF	Mean Sq.	T.F.	F	%P
L	36.57	2	18.28	15.23	121.88	18.32
D	102.12	2	51.06	42.55	340.34	53.49
S	40.09	2	20.04	16.70	133.62	20.21
D*L	1.06	4	0.26	0.22	1.77	-
S*L	2.70	4	0.67	0.56	4.51	-
S*D	2.66	4	0.66	0.55	4.44	-
Pooled Error	1.20	8	1.20			7.95
Total	186.425		91.0036			100

S=0.740448, R-Sq=94.1% and R-Sq adj) =92.4%

[Downloaded from railway.iust.ac.ir on 2024-10-10]

[DOI: 10.22068/ijmse.14.2.71]

The measure of degree of fit is based on the coefficient of determination (R2). When R2 approaches to unity, good response model results and it fits the actual data. The value of R-Sq (adj)=97.5% for base alloy and R-Sq (adj)=92.4% for composites are close to unity and hence acceptable.

3. 3. Effects of Variables on the Wear Rate

Fig. 3 (a and b) show the main effects plot for different parameters on wear rate of both base alloy and composite material. As observed from the plot, if the parameter line is nearer to mean line, that parameter tends to have less significant effect on wear rate. The parameter line having steep inclination from the mean line is having the highest significant effect on wear rate. It is observed from Fig. 3 (a and b) that, the parameter line of sliding distance (D) is steeper than other two parameters, namely sliding speed (S) and applied load (L). Hence, the influence of sliding

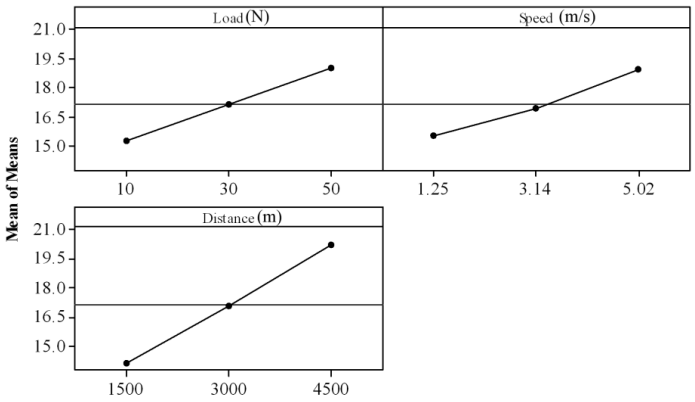

3.(a)

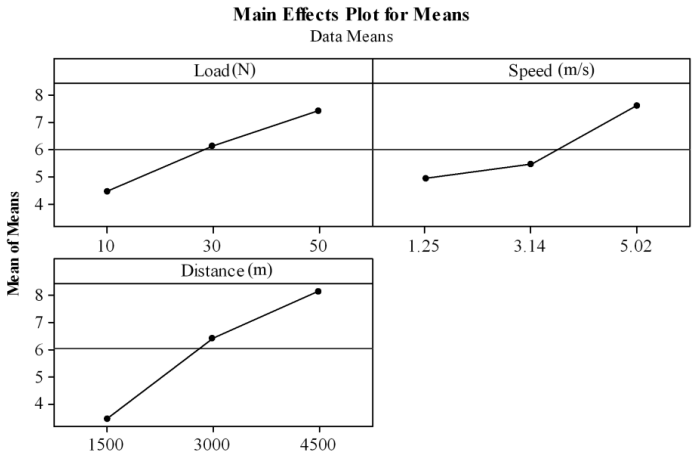

3.(b)

Fig. 3. Main effects plot of different parameters on wear rate of (a) base alloy and (b) composite

[Downloaded from railway.iust.ac.ir on 2024-10-10]

[DOI: 10.22068/ijmse.14.2.71]

distance on wear rate is more than the sliding speed and applied load for both the materials. The increase in sliding distance increases the wear rate of the specimen.

The wear rate was more for the base alloy when compared with composite. It indicates that more material was removed from the specimen in the absence of the reinforcement. It is observed from Fig. 3a, that the influence of sliding speed and applied load on wear rate was more in case of base alloy than the composite (Fig. 3b). When sliding speed and applied load were increased in the case of base alloy, it increased the contact surface between the disc and specimen, which in turn increased the friction between them. This resulted in removal of more material from the specimen.

In composite material similar mechanism was observed, but the contact surface between the disc and specimen was reduced as the reinforcements were projected from the specimen surface resulting in less friction. SiC_p acts as a load bearing member which reduces the wear rate of the composite at higher applied load. At higher sliding speed and applied load, graphite acts as a solid lubricant film on tribo-surface which reduces the coefficient of friction between metals. Similar mechanism was observed from earlier researchers [22-25].

3. 4. Interaction Factors on Wear Rate

The interaction plots of variables of the base alloy and composite are shown in Fig 4 (a and b). From Fig. 4a, it is observed that sliding distance has more significant effect on both base alloy and composites followed by sliding speed and applied load.

The sliding distance was the most significant factor influencing the wear rate of the base alloy and composites because, the parameter sliding distance had highest inclination, while the sliding speed and applied load had lowest influence. As observed from Fig. 4b, initially the wear rate decreases and further increasing the applied load and sliding speed which increases the wear rate.

3. 5. Multiple Linear Regression Equation

The multiple linear regression equation was developed using Minitab-16. The linear equations for base alloy and composite material were generated based on individual variable impacts and interaction between the variables. The equations 4.1 and 4.2 represent the regression equations for base alloy and composite material respectively. The positive value of the co-efficient suggests that the dry

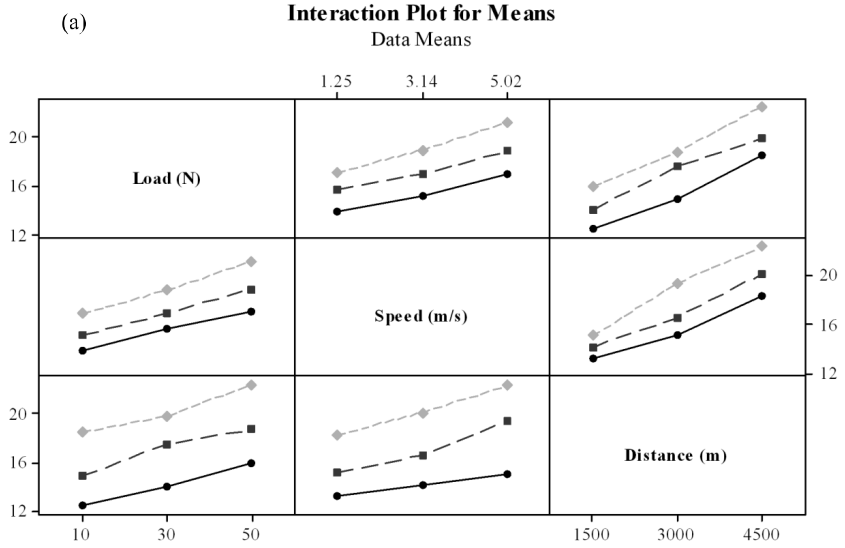

Fig. 4 (a). Interaction factors of wear rate for base alloy

[Downloaded from railway.iust.ac.ir on 2024-10-10]

[DOI: 10.22068/ijmse.14.2.71]

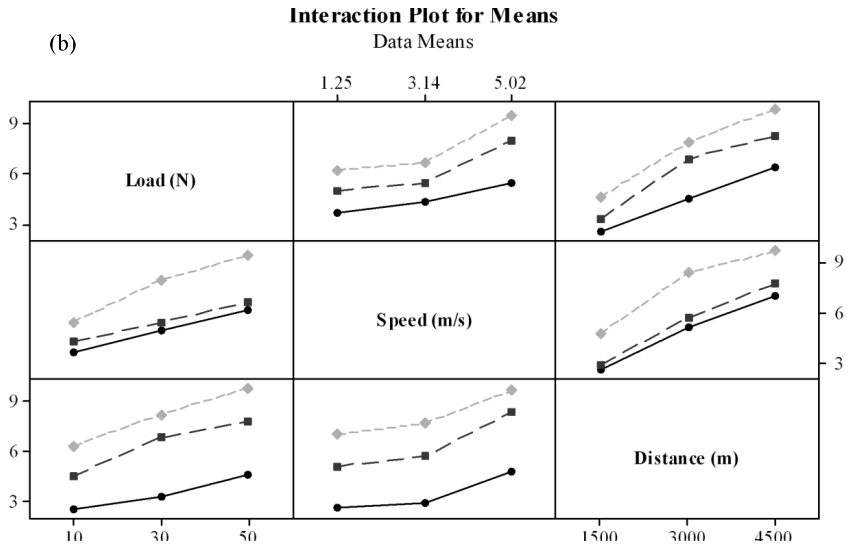

Fig. 4 (b). Interaction factors of wear rate for composite

sliding wear rate increases with increase in their associated variables, where as the negative values of the co-efficient suggest that the wear rate decreases with the increase in associated variables.

Wear (Base Alloy)= 8.15+0.641S+5.3 e^{-3}L+ 1.34e^{-3}D+7.51e^{-3}S*L+4.4e^{-5}S*D+1.9e^{-5}L*D (4.1)

Wear (composite)= -0.78+0.133S+2.57 e^{-2}L+ 1.07e^{-3}D+9.51e^{-3}S*L+1.24 e^{-4}S*D+4e^{-6}L*D (4.2)

All the interactions have positive effect on wear rate. The maximum interaction variable is obtained for applied load. From equations 5.1 and 5.2, the sliding distance impact on base alloy was 0.00134 and for composites it was 0.00107. The magnitude of wear rate of base alloy was more compared to the composite. The parameter associated with sliding speed and applied load and interaction between the parameters is positive. This suggests that, increase in these variables increases the wear rate of the materials for both base alloy and composites.

4. DISCUSSION

4. 1. Wear Mechanism

Fig. 5 shows SEM micrographs of worn out surfaces of base alloy and composite. Fig. 5(a) shows shallow grooves at lower applied load of 10 N and deep grooves (Fig. 5b) were formed as applied load was increased to 50 N, since it causes undergoes plastic deformation leading to severe wear. In base alloy, increasing of sliding speed increases the interfacial temperature between specimen and disc resulting in increase in the oxidation of the base alloy. During sliding, larger shear strain is induced on the surface of the specimen. This shear strain tends to induce the dislocations to glide along slip planes on the surface. This creates a fragmented eutectic phase on the surface and forms hardened surface layer on the specimen. This hardened layer contains a fine mixture of iron and fragmented eutectic phase. The iron particles which originated from the steel disc during wear test (Fig. 5a) were observed. The adhesive nature of wear was observed followed by excessive removal of material from the specimen surface further resulting in delamination (Fig. 5b). The adhesive wear was confirmed by plate like wear debris structure with sharp edges (Fig. 6a).

Fig. 5c shows the surface of composites with

[Downloaded from railway.iust.ac.ir on 2024-10-10]

[DOI: 10.22068/ijmse.14.2.71]

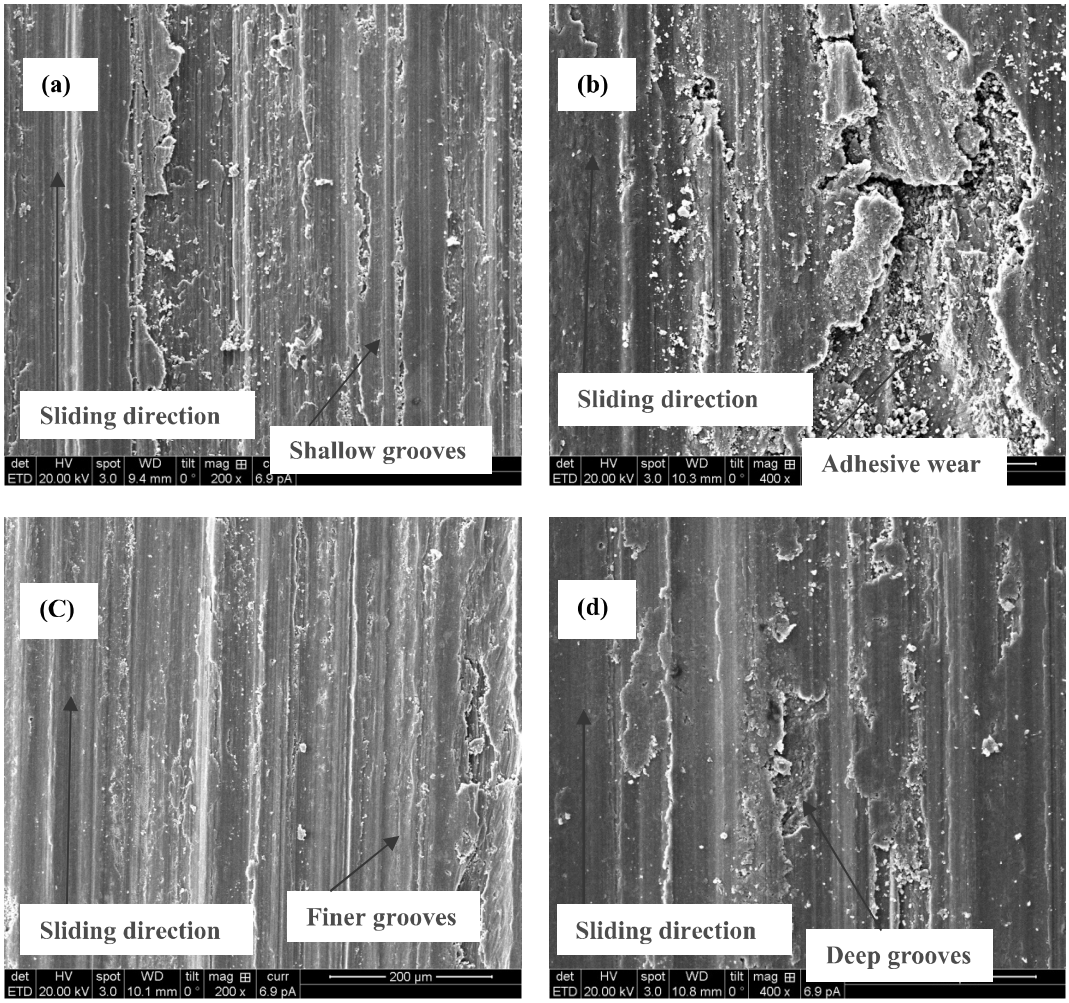

Fig. 5. SEM of worn out surfaces of base alloy (a). 10 N (b). 50 N and composite (c). 10 N (d). 50 N.

finer grooves and appears to be smooth when compared to the base alloy (Fig. 5a) due to the presence of reinforcements. At lower applied load of 10 N, wear rate of composites was lower when compared with the base alloy. As the applied load was increased to 50 N, the wear rate increased and formed deep grooves on the specimen surface of composite specimen (Fig. 5d). As the applied load was increased for base alloy, the layer formed on the contact surface of specimen was removed due to higher pressure resulting in more wear rate.

While in composites, the quantity of wear rate was low as the hardness of the composites was more than base alloy due to the addition of reinforcements that improves the tribological property of the composites (Table 2). In composites, the presence of SiC_p provides abrasion resistance and smearing of graphite on surface of specimen forms a tribolayer due to self lubricating property.

At an applied load of 10 N the asperities that are not able to resist the shear force deform and fill the valley and part of the asperities fracture. In addition, the projected SiC_p along with graphite detaches itself from the surface of the specimen. As the sliding distance increases, the fractured SiC_p lies between the specimen and steel disc that acts as an abrasive medium. They plough the surface of the specimen causing wear by the removal of small fragments of specimen. Hence, wear rate increases linearly during the initial stage of sliding distance. As sliding distance increases further, SiC_p which are rigidly

[Downloaded from railway.iust.ac.ir on 2024-10-10]

[DOI: 10.22068/ijmse.14.2.71]

held on to the specimen are subjected to less wear. The ratio of contact area of the base alloy to that of SiC_p with the counter face decreases. Hence, SiC_p takes more load and resists wear for longer time in comparison to the base alloy. At higher sliding distance, wear rate decreases. This result agrees well with the earlier researchers [33-35].

For the composites, at initial sliding speed (1.25 and 3.14 m/s) the wear rate decreases, but at higher sliding speed (5.02 m/s) the wear rate increases. When SiC_p in the composite specimen wear the steel disc, iron particles from the steel disc forms iron oxides (Fe_2O_3). Due the higher hardness of steel disc compared to the base alloy, the powdered and crushed SiC_p penetrates into the matrix of the composite specimen. However, the SiC_p present inside the matrix will resist the penetration of crushed SiC_p into the matrix [13, 18-25]. disc, oxides of aluminium from the specimen and graphite are mixed forming MML [36-37]. SEM (Fig. 6) shows the wear debris of worn out surfaces of the base alloy and composites.

The smeared SiC_p are crushed at the interface and powders of SiC_p are formed. At places where graphite particles are present, the SiC_p penetrates into the matrix easily due to lower hardness that result in squeezing of graphite particles from the matrix. The smeared graphite particles reduce the friction and heat generation. Fig. 5d shows the smearing of graphite at an applied load of 50 N. The powdered SiC_p along with ferrous oxides from the steel.

The wear debris of base alloy (Fig. 6a) are larger and in the form of thin sheets. This indicates that the base alloy has undergone significant plastic deformation. The wear debris in composites (Fig. 6b) is finer than the base alloy (Fig. 6a). The presence of smaller particles indicates that severe wear was not observed exhibiting mild wear in composite specimen. This is due to the presence of reinforcements that scatter in the matrix material minimizing the size of the wear debris. At longer sliding distance, a stable tribolayer on composite reduces the wear rate. The unstable tribolayer results in metal-to-metal contact that leads to increase in the wear rate of composites.

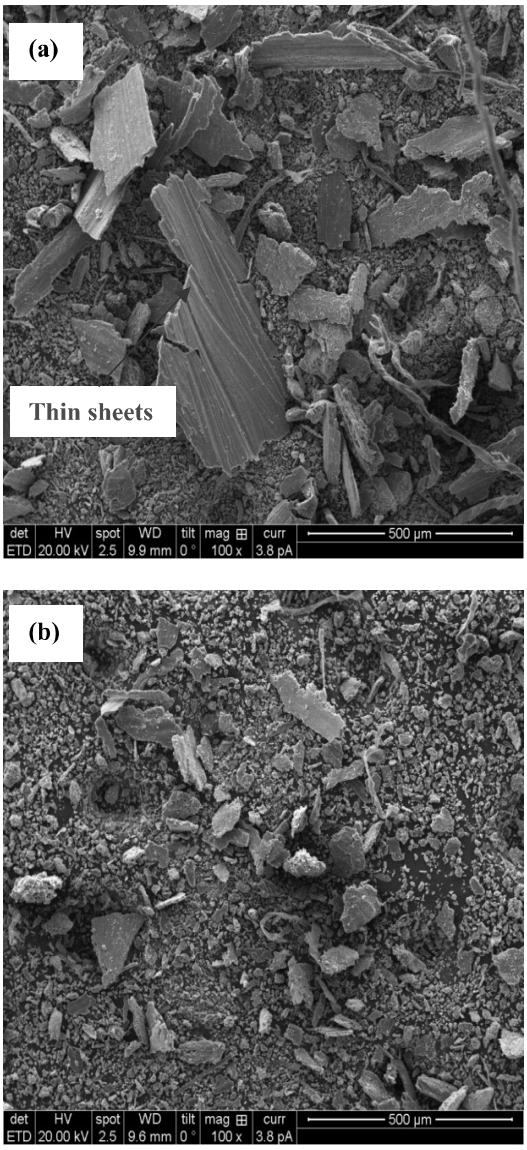

Fig. 6. SEM of wear debris (a). base alloy and (b). composite

EDS analysis of the worn out surface of base alloy and composites is shown in Fig. 7. The EDS analysis of the worn out surfaces of base alloy (Fig. 7a) shows low intensity of Si peak and high intensity of Al peak. The EDS of composites is shown in Fig. 7b. The 'C' peak is observed in Fig. 7b indicating the presence of graphite (solid lubricant). The moderate intensity of the 'Si' peak indicates that fractured SiC_p were noticed on specimen surface. However, a noticeable Fe peak

[Downloaded from railway.iust.ac.ir on 2024-10-10]

[DOI: 10.22068/ijmse.14.2.71]

is also observed (Fig. 7b) as the steel counterface material is abraded by the SiC_p. At higher loads, the hard SiC_p fractures and get trapped between steel counter face and the specimen.

The important factor affecting the dry sliding wear is the sliding speed and the associated co-efficient is negative in the regression equation (4.1 and 4.2). This suggests that the dry sliding wear rate decreases with increasing speed within the range of parameters studied. This has been attributed to the formation of MML and thus lowering the wear rate [33-37].

The fractured small particle of SiC_p between the specimen and the rotating disc forms third body abrasion. As the load increases, more SiC_p gets fractured. The brittle fracture of SiC_p in an irregular fashion leads to formation of new edges. The new edged particles will plough the material on the specimen. In case of SiC_p-Gr composite, the smeared graphite between the specimen and the rotating disc along with SiC_p serves to reduce the wear rate.

The iron particles abraded from the disc surface penetrate into the specimen. At higher sliding speed, the fractured particles squeeze out from the surface of composites forming a MML (Fig. 5d). These mechanisms are not present in the base alloy (Fig. 5 a and b). Similar mechanisms were observed by earlier researchers [3, 13, 22, 28 and 33].

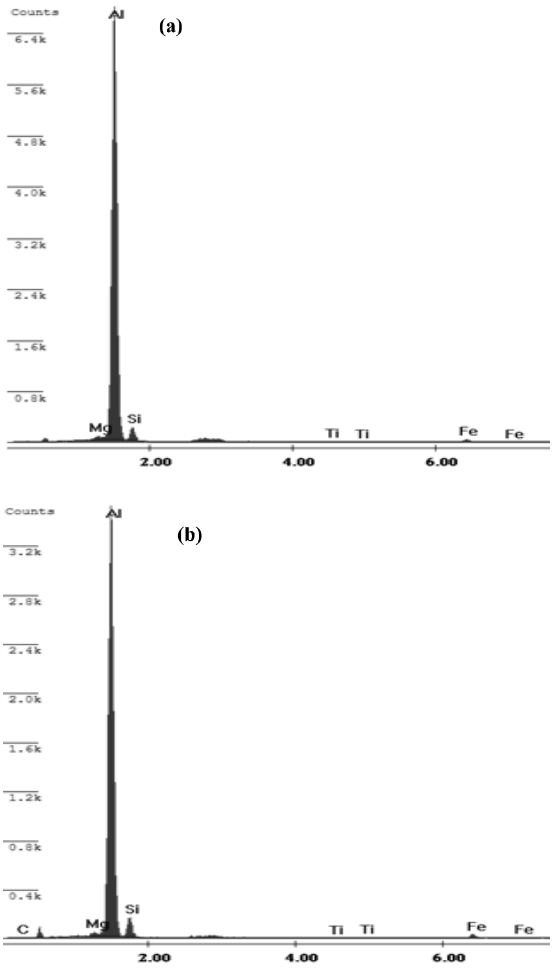

Fig. 7. EDS analysis of worn surfaces (a). base alloy and (b). Composite

4. 2. Sub-Surface Analysis of Worn-Out Surface

A comparison of the sequence of wear mechanism of the base alloy is shown as line diagram in Fig. 8 and SEM of the tested specimen (Fig. 9) is taken as evidence of the process. For the base alloy a large shear strain is induced in the subsurface region during sliding wear process. The magnitude of the surface strain increases with increasing sliding distance, sliding speed and applied load. Increasing of shear strain is closer to the surface; this shear strain induces the dislocation along the slip planes in subsurface region. This region is called as deformation zone as shown in Fig. 8a and it can be observed from the SEM (Fig. 9a). Consequently, eutectic region in the subsurface is fragmented and redistributed near the surface region. The formation of fragmented eutectic phase in the surface region leads to formation of hardened surface layer (Fig. 8b).

The thickness of layer depends on the varying parameters. The hardened layer contains a mixture of iron (Fe) and fragmented eutectic phase. The Fe originating from the steel disc is due to the transfer of metal across the steel disc during dry sliding wear process. That is evident from the SEM subsurface as shown in Fig. 9b. The Fe debris mixes mechanically with Al-Si base alloy during sliding.

Repeated sliding interface between steel disc and specimen results in formation of cracks and leads to delamination from the specimen surface (Fig. 8c) and is evident from the SEM subsurface

[Downloaded from railway.iust.ac.ir on 2024-10-10]

[DOI: 10.22068/ijmse.14.2.71]

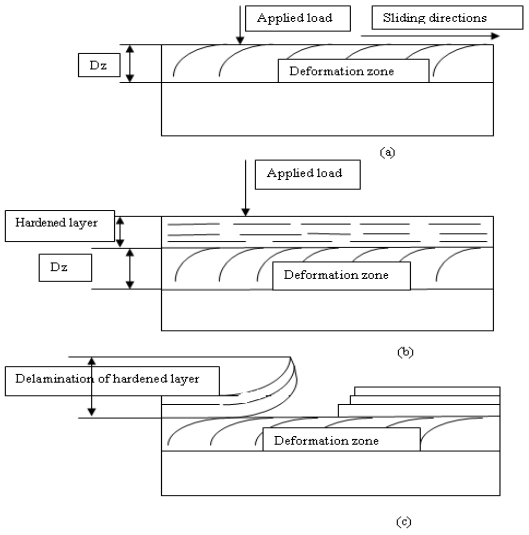

echanism of base alloy (a). formation of deformation zone (b). formati

layer (c). delamination of hardened layer

Fig. 8. Wear mechanism of base alloy (a). formation of deformation zone (b). formation of hardened layer (c). delamination of hardened layer

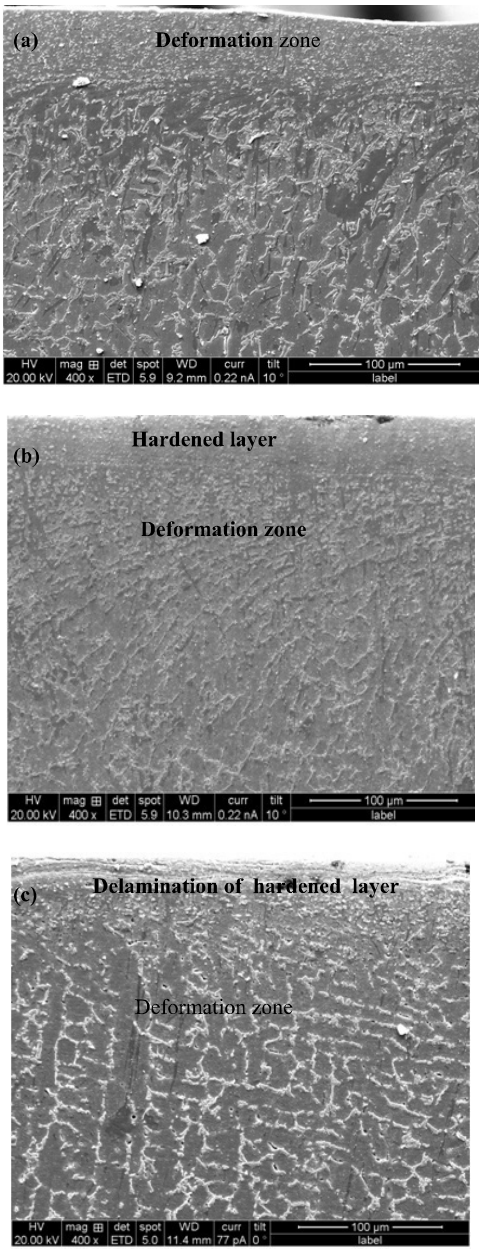

Fig. 9. SEM showing subsurface features in base alloy (a). formation of deformation zone (b). formation of hardened layer (c). delamination of hardened layer

(Fig. 9c). Decreased hardened layer at the top surface forms a delamination hardened layer in the vicinity of the top surface. Apart from this, the cracks are generated and propagate parallel to the surface of the specimen and nucleates at one point which results in removal of material as thin sheet like structure. From the SEM (Fig. 10), the material removed from the specimen adhered at the exit section leading to increase in the wear rate of the base alloy.

The wear mechanism of aged composite is shown in line diagram (Fig. 11) and is evident from the SEM (Fig. 12). In composites, the reinforcement acts as a barrier to the dislocation motion. The dislocation tends to pile up around the reinforcements. The pile-up of dislocations causes the fragmentation of SiC_p owing to the brittle nature of the SiC_P. The fractured SiC_p relives the shear strain in the deformed zone. The smeared Gr on the sub-surface region forms a solid lubricant film thereby resisting plastic deformation in the subsurface region. The fragmented SiC_p and Gr are redistributed in the surface of the hardened layer. This mechanism is shown in Fig. 11. The depth of the hardened layer of the composites is relatively less in comparison with that of the base alloy.

Fig. 11 shows the subsurface of A356-9SiC_p-

[Downloaded from railway.iust.ac.ir on 2024-10-10]

[DOI: 10.22068/ijmse.14.2.71]

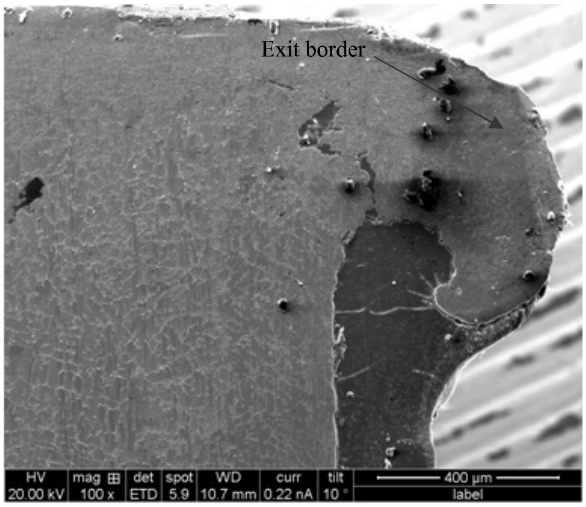

Fig. 10. Worn-out surfaces of base alloy at exit border

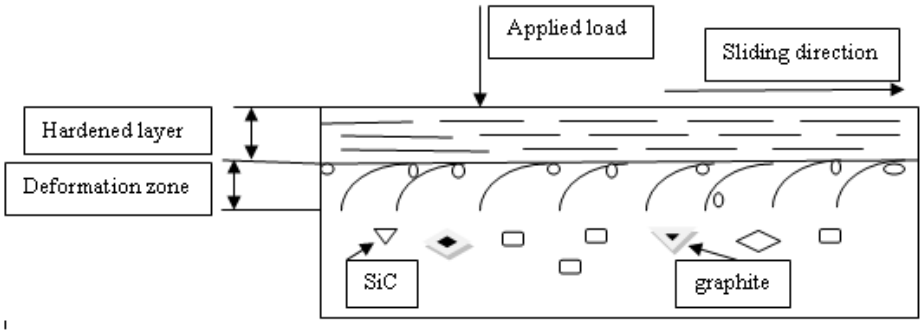

Fig. 11. Wear mechanism of composites

3Gr -9 hrs aged composites at a sliding speed 1.25 m/s where a hardened layer on the surface of the specimen is formed. Further increasing of sliding speed (5.02 m/s) increases the friction between specimen and rotating disc showing low deformation zone beneath the top surface and lower than this surface is the safe zone. The delamination was not observed on the surface of the specimen because of specimen containing reinforcement exhibiting superior hardness. It is evident from the SEM (Fig. 12 and Fig. 13).This results in resistance to flow of material from the specimen which reduces the wear rate of the composites when compared to the base alloy. For the composites, at initial sliding speed 1.25 m/s (Fig. 12) the wear rate decreases, but at higher sliding speed 5.02 m/s (Fig. 13) the wear rate increases.

Fig. 11 shows the smearing of Gr at an applied load of 50 N. The powdered SiC_p along with ferrous oxides from the steel disc, aluminium oxides from the specimen and Gr are mixed, forming MML [13, 33-37]. It is evident from the Fig. 12 and 13. The hardness of the MML is much higher than that of the specimen and the steel disc. This work-hardened layer reduces the wear rate and a stable, thin and hard MML formed on the surface of composite increases the wear resistance of the composite. It is evident from the SEM (Fig. 14) exit section that less flow of material is seen from the specimen surface.

The wear debris of the base alloy and composites is shown in Fig.15. The wear debris as observed from Fig. 15a are larger and is in the

[Downloaded from railway.iust.ac.ir on 2024-10-10]

[DOI: 10.22068/ijmse.14.2.71]

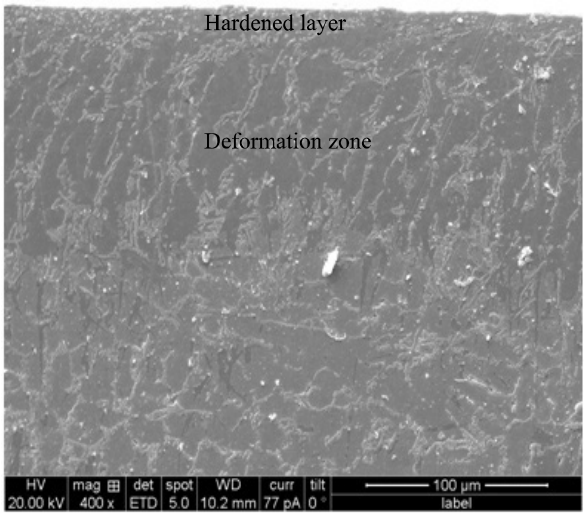

Fig. 12. SEM showing subsurface features in composites at sliding speed of 1.25 m/s

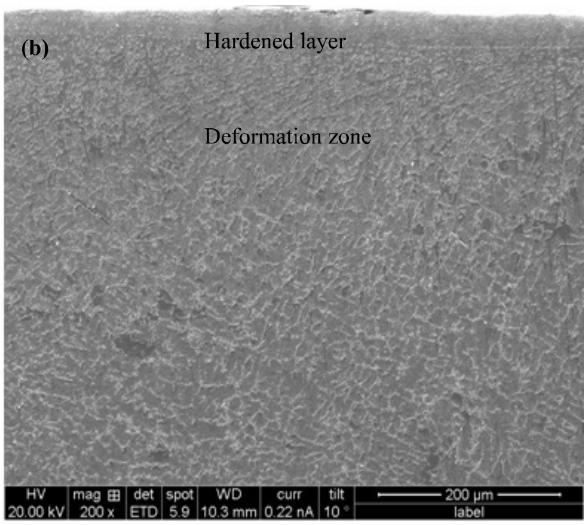

Fig. 13. SEM showing subsurface features in composites at sliding speed of 5.02 m/s

form of thin sheets. This indicates that the base alloy has undergone significant plastic deformation. As the applied load was increased for base alloy, the layer formed on the contact surface of specimen was removed due to higher pressure resulting in more wear rate. While in composites the quantity of wear rate was low. As the hardness of the composites is more than base alloy due to the addition of reinforcements which improves the tribological property of the composites. In composites, the presence of SiC_p provides abrasion resistance and smearing of Gr on sliding specimen surface forms a tribolayer due to self lubricating property.

The wear rate of composites increases with an increase in applied load. During initial stages of sliding, the asperities that are not able to resist the shear forces deform and fill the valley and part of the asperities fracture. In addition, the projected SiC_p along with Gr detaches itself from the surface of the specimen. As the sliding distance increases, the fractured SiC_p lies between the

[Downloaded from railway.iust.ac.ir on 2024-10-10]

[DOI: 10.22068/ijmse.14.2.71]

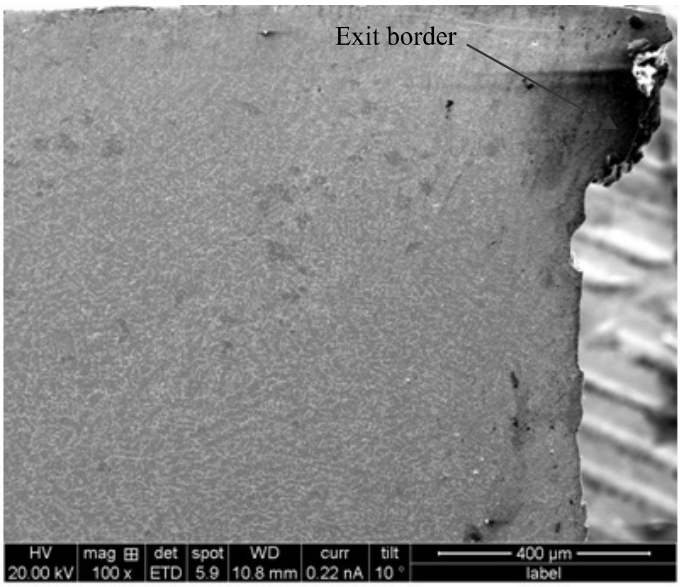

Fig. 14. Worn-out surfaces of composite at exit border

specimen and the counterface and act as an abrasive medium. They plough the surface of the specimen causing wear by the removal of small fragments of specimen material. Hence, wear rate increases linearly during the initial stage of sliding distance. As sliding distance increases further, SiC_p which were rigidly held to the specimen were subjected to less wear. The ratio of contact area of the base alloy to that of SiC_p with the counter face decreases. Hence SiC_p takes more load and resist wear for longer time in comparison to the base alloy. Hence, at higher sliding distance, wear rate decreses. These results agrees well with the general trend of wear behavior as suggested by earlier reasearchers [27-28,35].

The wear debris in composites (Fig. 16) is finer than the base alloy (Fig. 16). The presence of particles indicate that severe wear was not observed exhibiting mild wear in composite specimen. This is due to the reinforcements scattered in matrix material minimises the size of the wear particles. It reduces the wear rate of the composites when compared to the base alloy [33-34]. The wear rate increases for base alloy with an increase of sliding distance. While at longer sliding distance a stable tribolayer on composite

15.(a)

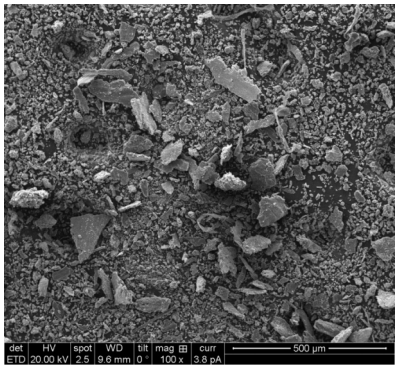

15.(b)

Fig. 15. SEM of wear debris (a) base alloy and (b) composite

[Downloaded from railway.iust.ac.ir on 2024-10-10]

[DOI: 10.22068/ijmse.14.2.71]

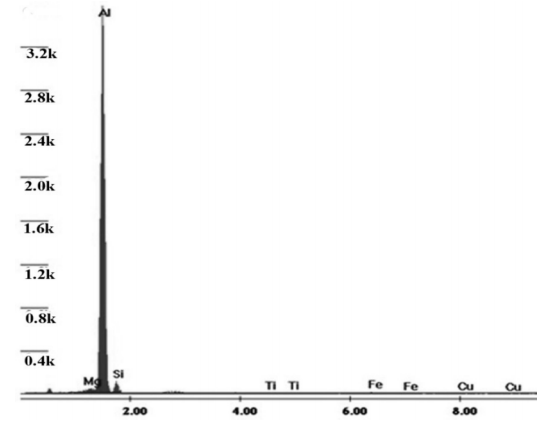

(a)

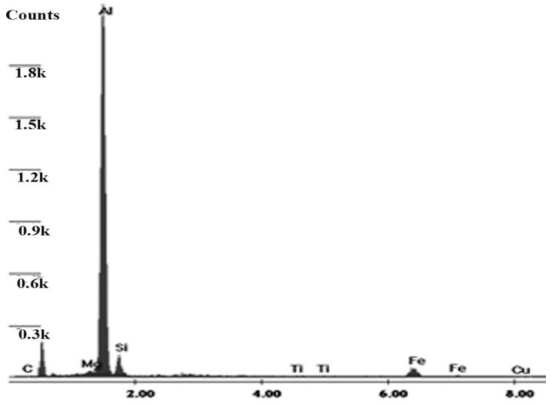

(b)

Fig. 16. EDS analysis of worn out surfaces (a) base alloy and (b) composite

reduces the wear rate. The unstable tribolayer leads to metal-to-metal contact that leads to increase in wear rate of composites.

EDS analysis of the worn out surfaces of base alloy and composites is shown in Fig.16. The EDS analysis of the worn out surfaces of base alloy (Fig. 16a) shows a low intensity of Si peak and high intensity of Al peak. The high Al peak indicates plastic deformation of base alloy during sliding. The EDS spectrum of composites is shown in Fig. 16b. The 'C' peak is observed in Fig. 16b, that indicates the presence of Gr (solid lubricant). The moderate intensity of the 'Si' peak indicates that fractured SiCp was noticed on specimen surface. However, a noticeable Fe peaks is also observed (Fig. 16b) as the steel counter surface material is abraded by the SiC_p. At higher loads, the hard SiC_p fractures and get trapped between steel counter face and the specimen.

The iron from the rotating disc is abraded by the fractured SiC_p, and Fe particles penetrate the surface of the specimen. At higher sliding speed, the fractured particles squeeze out onto the surface of composites forming a mechanical mixed layer (MML) (Fig.16b), these mechanisms are absent in the base alloy (Fig. 16a). The similar mechanism was observed from the earlier researchers [5, 28-37].

5. CONCLUSIONS

The following conclusions were drawn from the experimental data using a statistical technique of ANOVA using Minitab software.

1. The composite aged at T6-9 hrs provides higher hardness and gives MMCs the superior wear resistance and improved tribological behavior when compared to the base alloy.
2. The most significant factor that influences the wear rate of base alloy was sliding distance (56.81%), sliding speed (21.21%) and applied load (17.25%) and interaction factor D*L (1.1%) had nominal effect. For composites sliding distance (53.49%), sliding speed (20.21%) and applied load (18.32%) were the significant factors while there was no significant effect of interactions. The sliding distance is the most significant factor that influences the wear rate for both base alloy and composites.
3. For base alloy a large shear strain is induced in the subsurface region during sliding wear process causing severe plastic deformation.
4. The fractured SiC_p relives the shear strain in the deformed zone. The graphite present in the sub-surface region can form solid lubricant films on the worn-out surfaces thereby resisting plastic deformation in the subsurface region.
5. The powdered SiC_p along with ferrous

[Downloaded from railway.iust.ac.ir on 2024-10-10]

[DOI: 10.22068/ijmse.14.2.71]

oxides from the counterface, aluminium oxides from the specimen and graphite are mixed, forming a mechanically mixed layer (MML) reduces the wear rate of the composites.

6. Wear debris reveals that base alloy exhibited thin plate like structures due to the plastic deformation of matrix. In composites fine particles emerged to forms a stable MML which reduces the wear rate of the composites.
7. It is confirmed by EDS analysis of the worn out surfaces of composites that the presence of reinforcements along with iron were observed.

REFERENCES

1. Rohatgi, P. K., "Metal Matrix Composites". Defence Science Journal, 1993, 43 (4), 323-349.
2. Surappa, M. K., "Aluminium Matrix Composites: Challenges and Opportunities". Sadhana., 2003, 28 (1&2), 319-334.
3. Tjong, S. C.,Wu, S. Q. and Liao, H. C., "Wear Behaviour of an Al-12% Si Alloy Reinforced with a low Volume fraction of SiC Particles." Composite Science and Technology., 1997, 57, 1551-1558.
4. Pramila Bai, B. N., "Dry Sliding Wear of A356-Al-SiC_p Composites". Wear., 157, 1992, 295-304.
5. Surappa, M. K, Prasad, S. V. and Rohatgi, P. K., "Wear and Abrasion of Cast Al-Alumina Particle Composites". Wear., 1982, 77, 295-302.
6. Ravikiran, A. and Surappa, M. K., "Effect of Sliding Speed on Wear behaviour of A356 Al-30 wt.% SiCp MMC". Wear., 1997, 206, 33-38.
7. Natarajan, N., Vijayarangan, S. and Rajendran, I., "Wear behaviour of A356/25SiC_p Aluminium Matrix Composites Sliding Against Automobile Friction Material". Wear., 2006, 261, 812-822.
8. Wilson, S. and Alpas, A. T., "Effect of Temperature on the Sliding Wear Performance of Al Alloys and Al Matrix Composites". Wear., 1996, 196, 270-278.
9. Zhan, Y. and Zhang, G., "The role of Graphite Particles in the high Temperature Wear of Copper hybrid Composites Against Steel". Materials and Design., 2006, 27, 79-84.
10. Akhlaghi, F. and Bidaki, A. Z., "Influence of Graphite Content on the Dry Sliding and Oil Impregnated Sliding Wear Behaviour of Al 2024-Graphite Composites Produced by In Situ Powder Metallurgy Method". Wear., 2009, 266, 37-45.
11. Yang, J. B., Lin, C. B., Wang, T. C. and Chu, H. Y., The Tribological Characteristics of A356.2Al Alloy/Gr(P) Composites. Wear., 2004, 257, 941-952.
12. Liu, Y. B., Hu, J. D., Cao, Z. Y. and Rohatgi, P. K., "Wear Resistance of laser Processed Al-Si-Graphite Composites". Wear., 1997, 206, 83-86.
13. Rajaram, G., kumaran ,S., Srinivasa Rao, T. and Kamaraj, M., Studies on high Temperature Wear and its Mechanism of Al-Si/Graphite Composite under Dry Sliding Conditions. Tribology International., 2010, 43 (11), 2152-2158.
14. Jinfeng, L., Longtao, J., Wu, G., Shoufu, T. and Chen, G., "Effect of Graphitic Particle Reinforcement on Dry Sliding Wear of SiC/Gr/Al Composites". Rare Metal materials and Engineering., 2009, 38, 1894-1898.
15. Guo, M. L. T. and Tsao, C. Y. A., "Tribological Behaviour of Self-Lubricating Aluminium /SiC /Graphite Hybrid Composites Synthesized by the Semi-Solid Powder-Densification Method". Composites Science and Technology., 2000, 60, 65-74.
16. Basavarajappa, S., Chandramohan, G., Prasanna Kumar, M., Ashwin, M. and Prabu, M., "Dry Sliding Wear behavior of Al 2219/SiCp-Gr Hybrid Metal Matrix Composites". JMEPEG., 2006, 668-674.
17. Suresha, S. and Sridhara, B. K., "Effect of Addition of Graphite Particulates on the Wear behaviour in Aluminium–Silicon Carbide-Graphite Composites". Materials and Design., 2010, 31, 1804-1812.
18. Ames, W. and Alpas, A. T., "Wear Mechanisms in Hybrid Composites of Graphite-20 Pct SiC in A356 Aluminium Alloy". Metallurgical and Materials Transaction., 1995, 26A, 85-98.
19. Riahi, A. R. and Alpas, A. T., "The role of Tribo- layers on the Sliding Wear behavior of Graphitic Aluminum Matrix Composites". Wear., 2001, 251, 1396-1407.

[Downloaded from railway.iust.ac.ir on 2024-10-10]

[DOI: 10.22068/ijmse.14.2.71]

20. Gomez De Salazer, J. M. and Barrena, M. I., "Influence of Heat treatments on the Wear behaviour of an AA6092/SiC_p Composite". Wear., 2004, 256, 286-293.
21. Lin, C. B, Chang, R. J. and Weng, W. P., "A Study on Process and Tribological behaviour of Al alloy/Gr.(P) Composites". Wear., 1998, 217, 167-174.
22. Benal, M. M. and Shivanand, H. K., "Effect of Reinforcement Content and Ageing Durations on Wear Characteristics of Al (6061) based Hybrid Composites". Wear., 2007, 262, 759-763.
23. Viswanatha, B. M., Prasanna Kumar, M., Basavarajappa, S., Kiran, T. S., "Efffect of Ageing on Dry Sliding Wear Behaviour of Al-MMC for Disc Brake". Tribology Industry., 2014, 36 (1), 40-48.
24. Mahdavi Soheil. and Farshad Akhlaghi., "Effect of SiC content on the Processing, Compaction Behavior and Properties of Al6061/SiC/Gr Hybrid Composites". Journal of Materials Science., 2011, 46 (5), 1502-1511.
25. Venkataraman, B. and Sunderarajan, G., "Correlation between the Characteristics of the Mechanically Mixed Layer and Wear behaviour of Aluminium Al-7075 alloy and Al-MMC's". Wear., 2000, 245;22-38.
26. Kiran. T. S., Prasanna Kumar, M., Basavarajappa, S. and Viswanatha, B. M., "Dry Sliding Wear behavior of Heat Treated Hybrid Composites using Taguchi". Materials & Design., 2014, 63, 294-304.
27. Dharmalingam, S., Subramanian, R., Somasundara Vinoth, K. and Anandavel B., "Optimization of Tribological Properties in Aluminum Hybrid Metal Matrix Composites using Gray-Taguchi Method". JMEPEG., 2011, 20 (8), 1457.
28. Sahin, Y., Tribological behaviour of Metal Matrix and its Composite. Materials and Design., 2007, 28, 348-1352.
29. Ravindran, P., Manisekar, K., Narayanasamy, P., Selvakumar, N. and Narayanasamy, R., "Application of Factorial Techniques to Study the Wear of Al Hybrid Composites with Graphite Addition". Materials and Design., 2012, 39, 42-54.
30. Suresha, S. and Sridhara, B. K., "Friction characteristics of Aluminium Silicon Carbide and Graphite hybrid composites. Materials and Design"., 2012, 34, 576-583.
31. Ravikiran, A. and Surappa, M. K., "Effect of sliding speed on wear beahaviour of A356 Al-30 wt.% SiC_p MMC". Wear., 1997, 206, 33-38.
32. Hashim, J., Looney, L. and Hashmi, M. S. J., "Metal Matrix Composites: Production by the Stir Casting Method". Journal of Materials Processing Technology., 1999, 92-93, 1-7.
33. Hashim, J., Looney, L., Hashmi, M. S. J., "The Enhancement of Wettability of SiC particles in Cast Aluminium Matrix Composites". Journal of Materials processing Technology., 2001, 119, 329-335.
34. Basavarajappa, S. and Chandramohan, G., "Application of Taguchi techniques to Study Dry Sliding Wear Behaviour of Metal Matrix Composite". Materials and Design., 2007, 28, 1393-1398.
35. Basavarajappa, S. and Chandramohan, G., "Dry Sliding Wear Behavior of Hybrid Metal Matrix Composites". Materials Science., 2005, 11 (3), 253-257.
36. Sahin, Y. and Ozdin, K., A model for the Abrasive Wear Behaviour of Aluminium based Composites, Materials and Design., 2008, 29,728-733.
37. Ravindran, P., Manisekar, K., Narayanasamy, P. and Narayanasamy, R., "Tribological Behavior of Powder Metallurgy-Processed Aluminium Hybrid Composites with the Addition of Graphite Solid lubricant". Ceramic International., 2013, 39, 1169-1182.
38. Rao, R. N., Das, S., Mondal, D. P. and Dixit, G., "Effect of Heat Treatment on the Sliding Wear Behavior of Aluminium alloy (Al-Zn-Mg) hard particle Composite. Tribology International", 2010, 43, 330-339.

[Downloaded from railway.iust.ac.ir on 2024-10-10]

[DOI: 10.22068/ijmse.14.2.71]